Journal of Applied Electrochemistry (2005) 35:1253–1264
DOI 10.1007/s10800-005-9037-3
© Springer 2005

Electrochemical promotion of the oxidation of propane on Pt/YSZ and Rh/YSZ catalyst-electrodes

N. KOTSIONOPOULOS and S. BEBELIS*
Department of Chemical Engineering, University of Patras, Patras, GR, 26504, Greece
*(*author for correspondence, tel.: +30-2610-969511, fax: +30-2610-997269, e-mail: simeon@chemeng.upatras.gr)*

Received 14 December 2004; accepted in revised form 13 April 2005

Key words: electrochemical promotion, NEMCA effect, platinum, propane combustion, propane oxidation, rhodium, YSZ, yttria-stabilized-zirconia

Abstract

The effect of electrochemical promotion (EP) or non-faradaic electrochemical modification of catalytic activity (NEMCA) was studied in the catalytic reaction of the total oxidation of propane on Pt and Rh films deposited on Y_2O_3-stabilized-ZrO_2 (or YSZ), an O^{2-} conductor, in the temperature range 420–520 °C. In the case of Pt/YSZ and for oxygen to propane ratios lower than the stoichiometric ratio it was found that the rate of propane oxidation could be reversibly enhanced by application of both positive and negative overpotentials (''inverted volcano'' behavior), by up to a factor of 1350 and 1130, respectively. The induced rate increase Δr exceeded the corresponding electrochemically controlled rate $I/2F$ of O^{2-} transfer through the solid electrolyte, resulting in absolute values of the apparent faradaic efficiency $\Lambda = \Delta r/(I/2F)$ up to 2330. The Rh/YSZ system exhibited similar EP behavior. Abrupt changes in the oxidation state of the rhodium catalyst, accompanied by changes in the catalytic rate, were observed by changing the O_2 to propane ratio and catalyst potential. The highest rate increases, by up to a factor of 6, were observed for positive overpotentials with corresponding absolute values of faradaic efficiency Λ up to 830. Rate increases by up to a factor of 1.7 were observed for negative overpotentials. The observed EP behavior is explained by taking into account the mechanism of the reaction and the effect of catalyst potential on the binding strength of chemisorbed reactants and intermediates and on the oxidative state of the catalyst surface.

1. Introduction

The rate and selectivity of catalytic reactions occurring on metal and metal-oxide porous catalyst-electrode films deposited on solid electrolytes can be reversibly affected in a very pronounced and controlled manner by polarizing of the catalyst-electrode. This phenomenon is known in the literature as electrochemical promotion (EP) [1] or non-faradaic electrochemical modification of catalytic activity (NEMCA effect) [2, 3], as induced rate changes can exceed the corresponding rate of ion transport through the solid electrolyte by several orders of magnitude [4, 5]. Electrochemical promotion is a general phenomenon which allows for *in situ* tuning of catalyst performance and has been reported for over 60 catalytic reactions on a large number of catalyst-electrodes (Pt, Rh, Pd, Ag, Fe, Ni, IrO_2, RuO_2, etc.) interfaced to a variety of solid electrolytes and mixed electronic-ionic conductors. Electrochemically promoted catalytic rates up to 150 times higher than open-circuit (unpromoted) rates have been reported for oxygen ion conductors [5]. Work in this area has recently been reviewed [4, 5].

The results presented in this work concern the EP of Pt and Rh catalysts for the reaction of propane combustion using Y_2O_3-stabilized-ZrO_2 (YSZ), an O^{2-} conductor, as active catalyst support. The catalytic combustion of hydrocarbons is an important technology for emission control (e.g. automotive exhausts) and for energy production in an economical and less-polluting way (decreased production of nitrogen oxides). Combustion of alkanes is relatively slow compared to the combustion of other hydrocarbons [6], for example alkenes, and has been the subject of study of a large number of works, focusing mainly on the combustion of methane or propane on supported platinum group metals. Primary C–H bond cleavage is the preferred reaction pathway for alkane combustion [7] and thus trends in reactivity can be clearly correlated with C–H bond strengths [8]. Propane combustion has been mainly studied on supported platinum catalysts which are well-known to be the most active for the combustion of

hydrocarbons containing more than one carbon atom [8, 9]. Most of these studies concern the investigation of the nature of the observed activity enhancement for propane combustion of supported Pt catalysts exposed to SO_2 [7, 9, 10] as well as the investigation of the effect of support [11–13] and of the addition of promoters [14].

Electrochemical promotion of alkane combustion has previously been studied in the catalytic systems of methane total oxidation on Pt/YSZ [15] and Pd/YSZ [16], ethane total oxidation on Pt/YSZ [17] and, recently, propane total oxidation on Pt/YSZ [18]. The latter study focused on the comparison of the EP behavior of propane and propene total oxidation reactions between 344 and 365 °C and under stoichiometric or fuel-lean gas phase composition. In the present work the electrochemical promotion of Pt/YSZ and Rh/YSZ catalyst-electrodes was studied for the reaction of propane total oxidation over a wider range of temperature and gas phase compositions, covering O_2 to C_3H_8 ratios lower than the stoichiometric ratio. For both catalysts it was found that application of either positive or negative overpotentials can result in increase of the catalytic rate exceeding by far the corresponding rate of oxygen ion transfer through the solid electrolyte. The measured rate enhancement ratio $\rho = r/r_o$ values, where r and r_o are the promoted and open-circuit (unpromoted) rate, are the highest reported so far in EP studies using oxygen ion conductors.

2. Experimental details

The atmospheric pressure continuous flow experimental apparatus used in this study has been described previously [5, 19]. Reactants were certified standards of propane in He and O_2 in He (L' Air Liquide and Messer), which could be further diluted by mixing with He (99.999%, L' Air Liquide). The flow of gases was controlled by a set of calibrated mass flowmeters (MKS 1259C controlled by an MKS 247C controller). The total flow rate (80–485 cm^3 (STP) min^{-1}) was also measured by using a bubble flowmeter.

Reactants and products were analyzed by on-line gas chromatography using a Shimadzu 14B gas chromatograph with a thermal conductivity detector, connected to a Hewlett Packard 3395 integrator. CO_2 and H_2O were the only products detected under the conditions of the experiments. The carbon mass balance closure in all EP experiments was better than 2%. The presence of H_2O in the products was verified but not quantified. A Porapak Q column (Alltech, 50/80 mesh range, 6′ length×1/8″ O.D.) was used for separation and analysis of O_2, CO_2 and propane at 60 °C. CO_2 concentration in the effluent from the reactor was also continuously monitored by means of an infrared (IR) analyzer (Model Binos 100, Emerson Process Management). The electrochemical measurements were carried out using a Princeton Applied Research 263A potentiostat-galvanostat. It is noted that the catalyst potential values reported in this work under closed-circuit conditions include an uncompensated ohmic drop component. However, this does not affect the discussion of the results and the conclusions.

Two types of atmospheric pressure continuous flow reactors were used. A "single chamber" reactor [5, 17, 20] was used in the case of Pt catalyst-electrodes and a "fuel cell type" reactor [5, 21] in the case of Rh catalyst-electrode. In the "single chamber" reactor an YSZ (ZrO_2 8% mol Y_2O_3) disc (Dynamic-Ceramic) of 3/4″ (19 mm) diameter and 1 mm (catalyst Pt1) to 2 mm (catalyst Pt2) thickness, on which were deposited the Pt catalyst-electrode on the one side and two auxiliary Au electrodes on the opposite side, was suspended in the interior of a closed at one end quartz tube of volume approximately 50 cm^3, where the reaction mixture was fed, via three gold wires mechanically pressed on the YSZ disk. These wires were also used as electron collectors or suppliers. The Pt working electrode and the Au counter electrode were deposited exactly opposite to each other and had the same geometric (superficial) area.

The "fuel cell type" reactor consisted of a closed at one end YSZ (ZrO_2 8% mol Y_2O_3) tube (Zircoa, Inc; 19.5 mm outer diameter, 2 mm wall-thickness, 15 cm length). In this reactor configuration the Rh catalyst-working electrode was deposited on the inner side of the YSZ tube, covering part of the inner bottom area and exposed to the reaction mixture, while two Pt auxiliary electrodes (counter and reference electrodes) were deposited on the outer bottom side exposed to ambient air [21], the counter electrode being to its most part opposite to the working electrode. The three electrodes were connected to the potentiostat-galvanostat via Au wires.

The Pt electrodes used in this study were deposited on the YSZ electrolyte by application of thin coatings of Engelhard M603B Pt paste followed by drying and calcination in air, first at 400 °C (4 °C/min) for 2 h and then at 840 °C (7 °C/min) for 30 min (catalyst Pt1) or at 800 °C (7 °C/min) for 20 min (catalyst Pt2). The Au counter and reference electrodes were deposited on the YSZ disk by application of thin coatings of Engelhard A1118 Au paste followed by drying and calcination in air, first at 400 °C (4 °C/min) for 2 h and then at 900 °C (7 °C/min) for 15 min. The Rh electrode was deposited on the YSZ electrolyte by application of thin coatings of Engelhard 8826 Rh paste followed by drying and calcination in air at 550 °C (3 °C/min) for 3 h. The procedure was repeated until the resistance of the catalyst film was less than approximately 1 kΩ. Before the beginning of each individual experiment the rhodium catalyst film was reduced under H_2/He mixture flow (1% H_2 in He for 1 h) at the temperature of the experiment. Both Pt and Rh catalyst-electrodes were porous with thicknesses on the order of a few μm, as shown using scanning electron microscopy. Typical scanning electron micrographs of Pt and Rh electrodes (before reduction) are presented in Figures 1 and 2,

respectively, where differences in crystallite size between the two electrodes can also be seen. Blank experiments showed that the catalytic rate of propane combustion on the solid electrolyte and on the Au auxiliary electrodes was negligible under the conditions of the present experiments.

The surface mol (mol of active sites) Pt or Rh of the catalyst films used in the present study, the corresponding true surface areas and the corresponding geometric (superficial) surface areas are presented in Table 1. The surface mol for each catalyst-electrode film were estimated by measuring the rate of ethylene oxidation under certain conditions ($T = 300$ °C, $P_{O_2} = 4.5$ kPa, $P_{C_2H_4} = 0.4$ kPa for Pt and $T = 370$ °C, $P_{O_2} = 1.3$ kPa, $P_{C_2H_4} = 7.4$ kPa for Rh) and then comparing under the same conditions the measured rate with the rate reported in Refs. [21] and [19], for the case of Rh and Pt, respectively, where the catalyst surface mol are also reported. The assumption of the same turnover frequencies (TOF) for ethylene oxidation, which is required for this calculation, is justified by the fact that the same precursors (metal pastes) and calcination procedures were used for the preparation of catalysts both in the present work and in the work described in the aforementioned references. The true surface areas of the catalyst films (Table 1) were estimated using as density of surface Pt and Rh atoms the one corresponding to Pt(111) and Rh(111) face, that is, 1.50×10^{15} cm^{-2} for Pt(111) and 1.60×10^{15} cm^{-2} for Rh(111), respectively. Differences in the true surface areas of the catalyst films (Table 1) are due mainly to the different amount of the deposited catalyst in each case.

3. Results

3.1. *Propane oxidation on Pt/YSZ*

The EP experiments were carried out in the temperature range 425–520 °C and for $P_{O_2}/P_{C_3H_8}$ ratios between 0.5

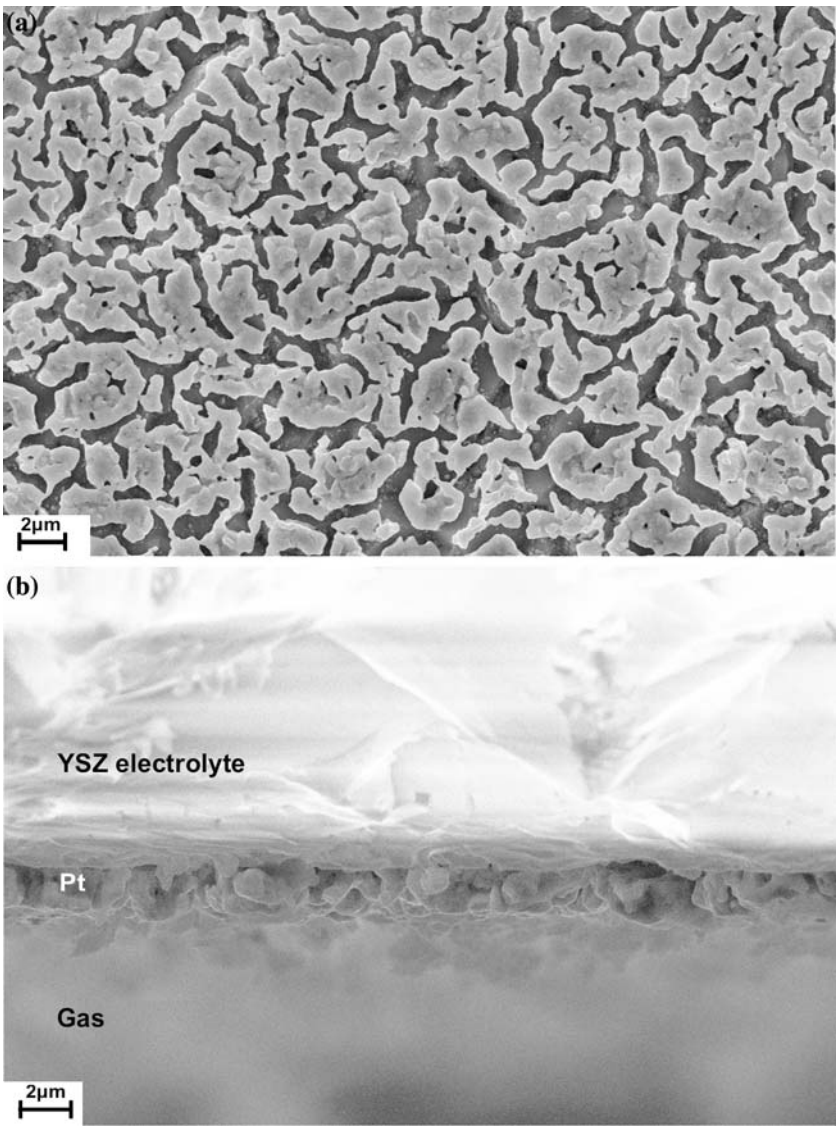

Fig. 1. Scanning electron micrographs (a) of the top side of a porous Pt catalyst-electrode film (b) of a section perpendicular to the Pt/YSZ interface. Catalyst Pt1.

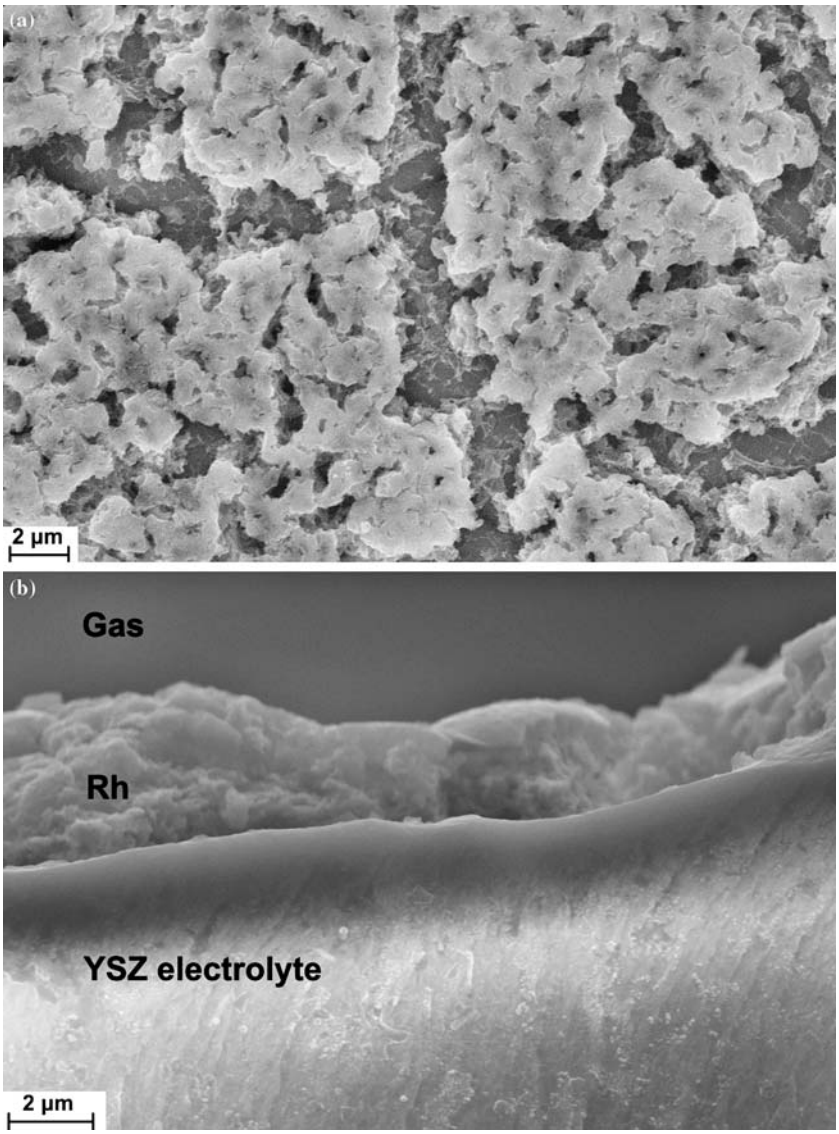

Fig. 2. Scanning electron micrographs (a) of the top side of a porous Rh catalyst-electrode film (b) of a section perpendicular to the Rh/YSZ interface.

Table 1. Surface mol (N), true surface areas (A) and geometric surface areas (A_g) of the catalyst films

Catalyst film	10^7 N(mol)	A (cm^2)	A_g (cm^2)
Pt1	1.0	40	2.0
Pt2	6.0	240	1.5
Rh	16	602	1.1

and 3.4. The total flow rate was between 95 and 485 cm^3 (STP) min^{-1}.

Figure 3a shows a typical galvanostatic transient, that is, it depicts the response of the catalyst potential U_{WR} and of rate r and turnover frequency (TOF) of propane oxidation on Pt (expressed in mol O s^{-1}) upon imposition of a constant positive current of 1.5 mA between the Pt catalyst (catalyst film Pt1, $N = 1.0\times10^{-7}$ mol Pt) and the Au counter electrode. The experiment was carried out at 425 °C and at fixed feed gas composition $P_{O_2} = 0.92$ kPa and $P_{C_3H_8} = 1.95$ kPa, that is, at a $P_{O_2}/P_{C_3H_8}$ ratio equal approximately to 0.5 (hydrocarbon-rich mixture). At the beginning of the experiment ($t < 0$) no current is applied ($I = 0$) and the open-circuit catalytic rate is $r_o = 1\times10^{-8}$ mol O s^{-1}, while the open-circuit catalyst potential $U_{WR,o}$ is equal to −376 mV. Then at $t = 0$ a constant current $I = 1.5$ mA is applied and O^{2-} are transferred from the YSZ support to the Pt catalyst-electrode at a rate $I/2F = 7.8\times10^{-9}$ mol O s^{-1}, where F is the Faraday constant. This causes an increase in the catalytic rate which after approximately 15 min stabilizes to a new value $r = 4.87\times10^{-7}$ mol O s^{-1}, which is 49 times higher than the open-circuit value (rate enhancement ratio $\rho = r/r_o = 49$). The corresponding steady-state value of catalyst potential U_{WR} becomes +197 mV. The rate increase $\Delta r = 4.77\times10^{-7}$ mol O s^{-1}

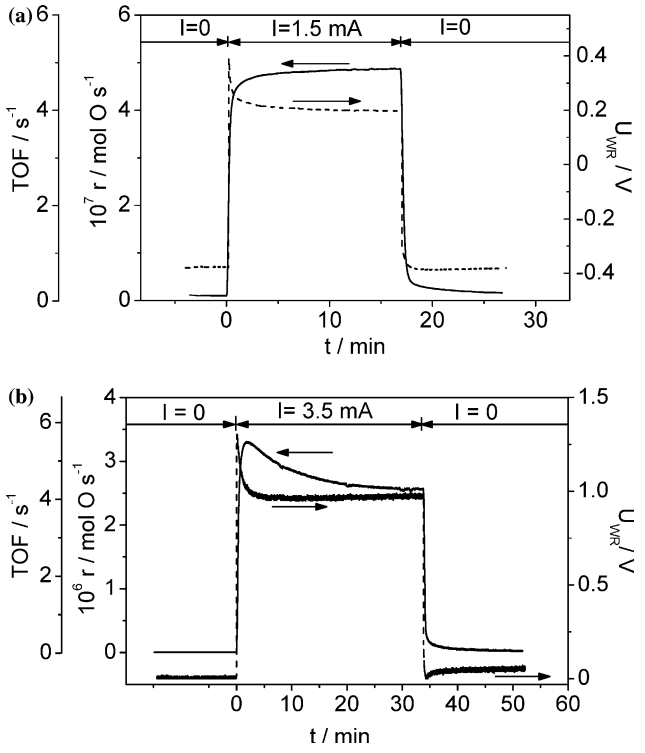

Fig. 3. Rate r, turnover frequency TOF and catalyst potential U_{WR} response to a step change in applied positive current. (a) Catalyst Pt1; $T=425$ °C; Feed composition: $P_{O_2}=0.92$ kPa, $P_{C_3H_8}=1.95$ kPa; Flow rate: 101 cm^3 (STP) min^{-1} (b) Catalyst Pt2; $T=480$ °C; Feed composition: $P_{O_2}=4.7$ kPa, $P_{C_3H_8}=1.4$ kPa; Flow rate: 483 cm^3 (STP) min^{-1} (see text for discussion).

is 61 times larger than the rate of O^{2-} supply $I/2F$, that is, each O^{2-} supplied to the catalyst causes, on the average, 61 additional chemisorbed oxygen atoms to react. Thus the system exhibits NEMCA behavior with corresponding enhancement factor or faradaic efficiency Λ equal to 61, where Λ is defined from [2–5]:

$$\Lambda = \Delta r/(I/2F) \quad (1)$$

In the promoted catalyst state the propane conversion is equal to 3.3% at a flow rate equal to 101 cm^3 (STP) min^{-1}.

The observed changes in catalytic rate and catalyst potential are reversible. Upon current interruption both the catalytic rate and catalyst potential return practically to their initial open-circuit values. The NEMCA relaxation time constant τ, defined [5, 19] as the time required for the rate change Δr to reach 63% of its steady-state value during a galvanostatic transient, is in the present case equal to 0.29 min. This value is very close to the time $2FN/I=0.22$ min, where $N=1.0\times10^{-7}$ mol Pt is the surface mol Pt of the catalyst film Pt1, that is, to the time required for the pumped ionic species to create a monolayer on the gas exposed surface. This is in agreement to the formation of an effective electrochemical double layer on the gas exposed catalyst surface as the origin of EP [2, 4, 5].

Figure 3b shows for another catalyst film (catalyst film Pt2, $N=6\times10^{-7}$ mol Pt) at a higher temperature (480 °C) and at a higher feed $P_{O_2}/P_{C_3H_8}$ ratio ($P_{O_2}/P_{C_3H_8}=3.4$) the response of the catalyst potential U_{WR} and of rate r and turnover frequency (TOF) of propane oxidation (expressed in mol O s^{-1}) upon application of a constant positive current of 3.5 mA. The observed behavior is similar to the one depicted in Figure 3a, however in this case the attained steady-state values of rate enhancement ratio $\rho=r/r_o$ and faradaic efficiency Λ are significantly higher. The rate enhancement ratio ρ at steady state is equal approximately to 1350 ($r_o=1.9\pm0.3\times10^{-9}$ mol O s^{-1} measured at 108 cm^3 (STP) min^{-1}, $r=2.56\times10^{-6}$ mol O s^{-1}), that is, the promoted catalytic rate r is at steady-state approximately 1350 times higher than the open-circuit rate r_o. This is a very spectacular increase in the rate, in view also of the fact that the highest ρ value reported so far in literature for oxygen ion conductors is 150 [5]. The corresponding steady-state faradaic efficiency Λ value is equal to 141. In the promoted catalyst state the propane conversion is equal to 5.1% at a flow rate equal to 483 cm^3 (STP) min^{-1}. Upon current interruption both the catalytic rate and the catalyst potential tend to relax to their initial open-circuit values.

Figure 4a shows for catalyst film Pt1 and for $P_{O_2}/P_{C_3H_8}\approx0.5$ the steady-state effect of applied potential on the catalytic rate enhancement ratio $\rho=r/r_o$ in the temperature range 425–485 °C. As shown in the figure, the rate of propane oxidation increases significantly, up to 54 times, upon positive overpotential application, while a less pronounced increase, up to 1.8 times ($T=450$ °C), is observed for negative overpotentials. This behavior is known as 'inverted volcano behavior' [5, 22] and according to the recently identified rules of EP [5, 22, 23] it is generally expected when both the electron acceptor (oxygen) and electron donor (propane) reactants are present on the catalyst surface at low coverages. The maximum propane conversion observed here under potential application was 5% (at 485 °C) at a flow rate equal to 100 cm^3 (STP) min^{-1}.

In Figure 4b is depicted the steady-state effect of applied potential U_{WR} on the catalytic rate enhancement ratio $\rho=r/r_o$ for catalyst film Pt2 at $P_{O_2}/P_{C_3H_8}\approx3.1$ and in the temperature range 480–520 °C. Similar behavior is observed, however in this case the rate enhancement ratios ρ are significantly higher, up to 1270 ($T=480$ °C) for positive overpotentials and up to 1130 ($T=480$ °C) for negative overpotentials. These rate enhancement ratios exceed by almost one order of magnitude the ones reported so far in literature for EP studies using oxygen ion conductors as active catalyst supports [5]. The highest measured propane conversion in the promoted catalyst state was equal to 20.3% at 520 °C and a flow rate of 102.5 cm^3 (STP) min^{-1} (the open-circuit propane conversion at the same conditions was equal to 0.2%). It is noticed that under the conditions of Figure 4b the maximum observed rate enhancement ratio values at each individual temperature

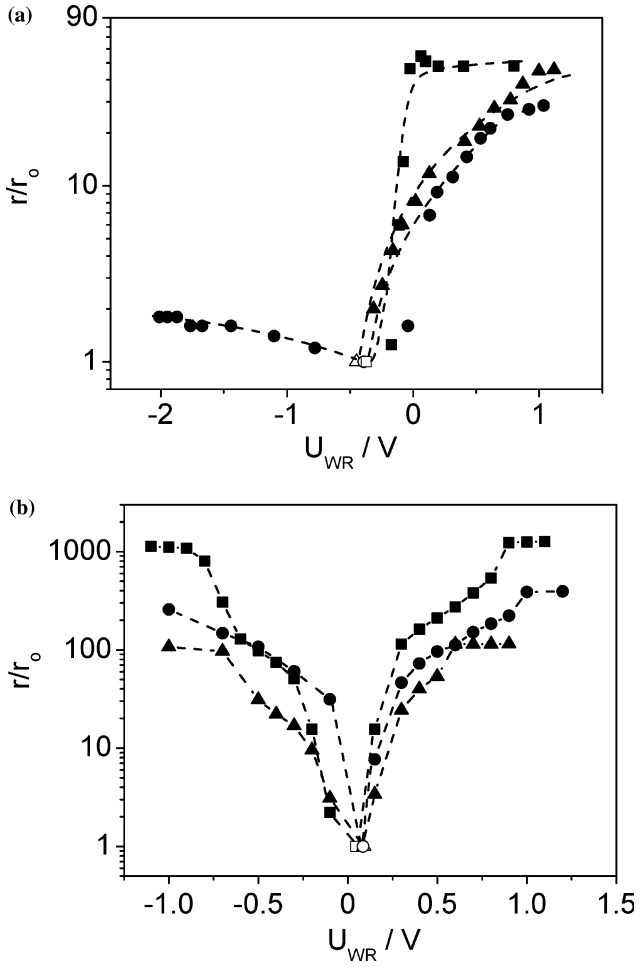

Fig. 4. Steady-state effect of applied potential U_{WR} on the catalytic rate enhancement ratio $\rho = r/r_o$ at different temperatures. Open symbols correspond to open-circuit conditions. (a) Catalyst Pt1; Conditions: $P_{O_2} = 0.92$ kPa, $P_{C_3H_8} = 1.95$ kPa; Flow rate: 95–101 cm^3 (STP) min^{-1}; Key for T: (■) 425 °C ($r_o = 1\times10^{-8}$ mol O s^{-1}, $U_{WR,o} = -371$ mV), (●) 450 °C ($r_o = 1.25\times10^{-8}$ mol O s^{-1}, $U_{WR,o} = -391$ mV), (▲) 485 °C ($r_o = 1.75\times10^{-8}$ mol O s^{-1}, $U_{WR,o} = -448$ mV) (b) Catalyst Pt2; Conditions: $P_{O_2} = 4.7$ kPa, $P_{C_3H_8} = 1.5$ kPa; Flow rate: 95–105 cm^3 (STP) min^{-1}; Key for T: (■) 480 °C ($r_o = 2.3\times10^{-9}$ mol O s^{-1}, $U_{WR,o} = 45$ mV), (●) 500 °C ($r_o = 7.6\times10^{-9}$ mol O s^{-1}, $U_{WR,o} = 85$ mV) (▲) 520 °C ($r_o = 25.4\times10^{-9}$ mol O s^{-1}, $U_{WR,o} = 90$ mV).

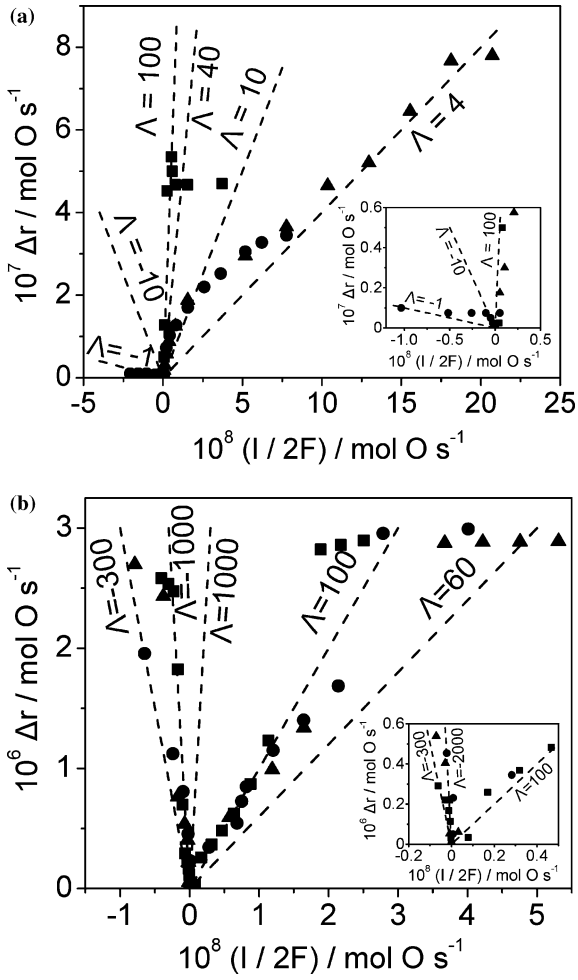

Fig. 5. Steady-state effect of applied current I on the induced change in the rate of propane oxidation Δr (expressed in mol O s^{-1}). Dashed lines are constant Faradaic efficiency Λ lines. (a) Catalyst Pt1 (b) Catalyst Pt2. Conditions as in Figure 4.

did not differ significantly for positive or negative overpotential application. This behavior differs from the one presented in Figure 4a, where the induced rate increase ($T = 450$ °C) is more pronounced for positive overpotentials. The difference can be attributed to the corresponding different $P_{O_2}/P_{C_3H_8}$ ratios and temperature range, that is, to differences in the ratio of the coverage of the adsorbed reactants and in the oxidative state of the catalyst surface, as discussed below.

Figures 5a and 5b show for catalyst films Pt1 and Pt2 and for the conditions of Figure 4a ($P_{O_2}/P_{C_3H_8} \approx 0.5$, temperature range 425–485 °C) and Figure 4b ($P_{O_2}/P_{C_3H_8} \approx 3.1$, temperature range 480–520 °C), respectively, the steady-state effect of applied current I or, equivalently, of corresponding rate $I/2F$ of O^{2-} transfer through the solid electrolyte on the observed increase in the catalytic rate Δr (expressed as total oxygen consumption, in mol O s^{-1}) due to the EP of the catalytic reaction. Dashed lines are constant Faradaic efficiency Λ lines. Under the conditions of Figure 5a, faradaic efficiency Λ values from −10 (Figure 5a, inset) to 175 were measured. Under the conditions of Figure 5b the measured absolute values of Λ were higher. Λ values from approximately 40–730 (typically from 40 to 200) were measured for positive currents and from approximately −300 to −2330 for negative currents. The highest absolute value of Λ ($\Lambda = -2330$) was measured at 480 °C for application of −300 mV corresponding to a current of −9.5 μA.

3.2. *Propane oxidation on Rh/YSZ*

The EP experiments were carried out in the temperature range 460–500 °C. The total flow rate was between 80 and 105 cm^3 (STP) min^{-1}. As shown below, the EP of propane combustion on Rh/YSZ presents similar characteristics to the case of propane combustion on Pt/YSZ. However in this case the change in the oxidative state of rhodium catalyst surface with changing gas

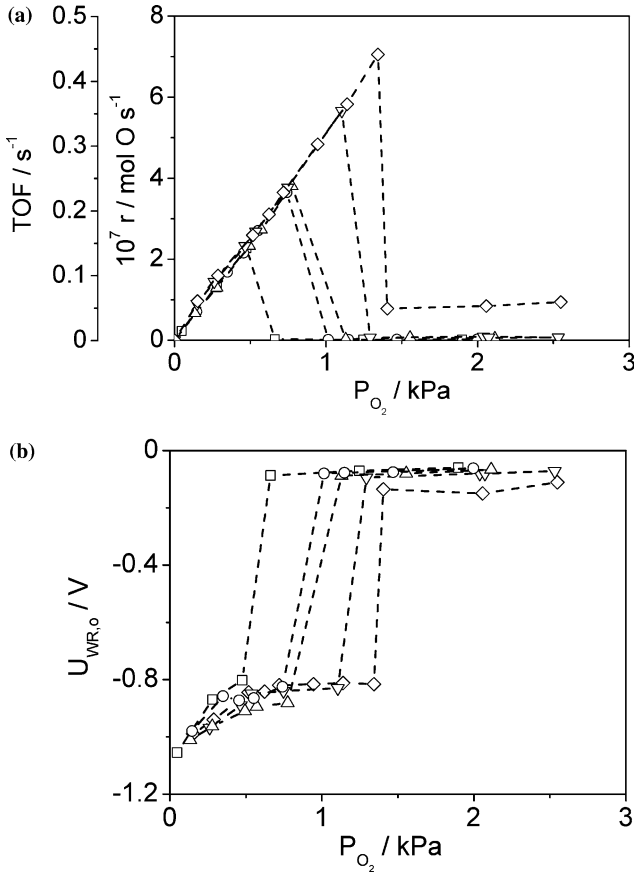

Fig. 6. Dependence of the open-circuit rate r of propane oxidation (expressed as O consumption rate, in mol O s^{-1}) and turnover frequency (TOF) (a) and of the open-circuit catalyst potential $U_{WR,o}$ (b) on oxygen partial pressure P_{O_2} at constant $P_{C_3H_8}$ (2 kPa). Catalyst Rh; Key for T: (□) 420 °C, (○) 440 °C, (△) 460 °C, (▽) 480 °C, (◇) 500 °C; Flow rate: 80–93 cm^3 (STP) min^{-1}.

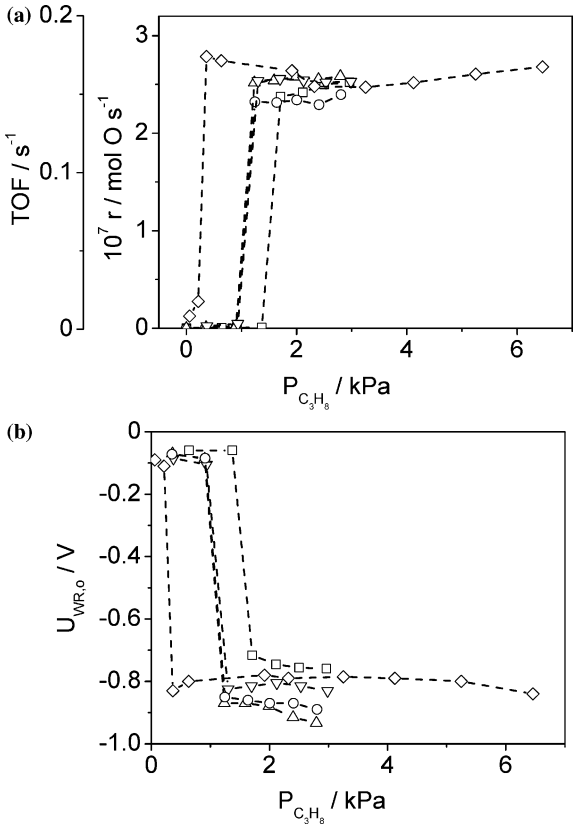

Fig. 7. Dependence of the open-circuit rate r of propane oxidation (expressed as O consumption rate, in mol O s^{-1}) and turnover frequency (TOF) (a) and of the open-circuit catalyst potential $U_{WR,o}$ (b) on propane partial pressure $P_{C_3H_8}$ at constant P_{O_2} (0.5 kPa). Catalyst Rh; Key for T: (□) 420 °C, (○) 440 °C, (△) 460 °C, (▽) 480 °C, (◇) 500 °C; Flow rate: 80–105 cm^3 (STP) min^{-1}.

phase composition, temperature and catalyst potential mainly determines the observed EP behavior.

Figure 6 shows for catalyst film Rh the effect of oxygen partial pressure P_{O_2} on the rate r of propane oxidation (Figure 6a) and on the open-circuit catalyst potential $U_{WR,o}$ (Figure 6b), at constant $P_{C_3H_8} = 2$ kPa. The rate first increases with increasing P_{O_2} and then, at a critical oxygen partial pressure value, hereafter denoted by $P^*_{O_2}$, decreases abruptly (Figure 6a). The abrupt rate decrease is accompanied by an abrupt increase in the open-circuit catalyst potential $U_{WR,o}$ (Figure 6b), by approximately 750 mV. The critical oxygen partial pressure $P^*_{O_2}$ shifts to higher values with increasing temperature.

Figure 7 shows the effect of propane partial pressure $P_{C_3H_8}$ on the rate r of propane oxidation (Figure 7a) and on the open-circuit catalyst potential $U_{WR,o}$ (Figure 7b), at constant $P_{O_2} = 0.5$ kPa. By decreasing $P_{C_3H_8}$ the rate changes slightly until a critical propane partial pressure is reached, hereafter denoted by $P^*_{C_3H_8}$, at which the rate decreases abruptly to a much lower value (Figure 7a). This rate change is accompanied by an abrupt increase in open-circuit catalyst potential $U_{WR,o}$ (Figure 7b), by approximately 750 mV. The critical propane partial pressure $P^*_{C_3H_8}$ shifts to lower values with increasing temperature.

The behavior depicted in Figures 6 and 7 provides strong evidence that the abrupt open-circuit rate and potential transition is due to the formation of a surface rhodium oxide. Similar to the case of ethylene [21] and propylene [24] combustion on Rh/YSZ, the reduced surface exhibits significantly higher catalytic activity for propane oxidation as compared to the oxidized surface, which can lead to such abrupt rate and open-circuit potential variations near the surface oxide stability limit [5, 21, 24–26]. The assignment of the abrupt potential decrease to surface oxide formation is corroborated in Figure 8, where the oxygen activity a_O on the catalyst surface corresponding to the each data point in Figures 6b and 7b is compared to the oxygen activity values corresponding to the stability limits of the bulk oxides of rhodium [21, 27]. The oxygen activity a_O on the catalyst surface is related to the measured open-circuit potential $U_{WR,o}$ via the equation [5, 24]:

$$U_{WR,o} = (RT/4F)\ln[a_O^2/P_{O_2,R}] \quad (2)$$

where $P_{O_2,R}$ is the oxygen partial pressure over the reference electrode (for the Pt/air reference electrode

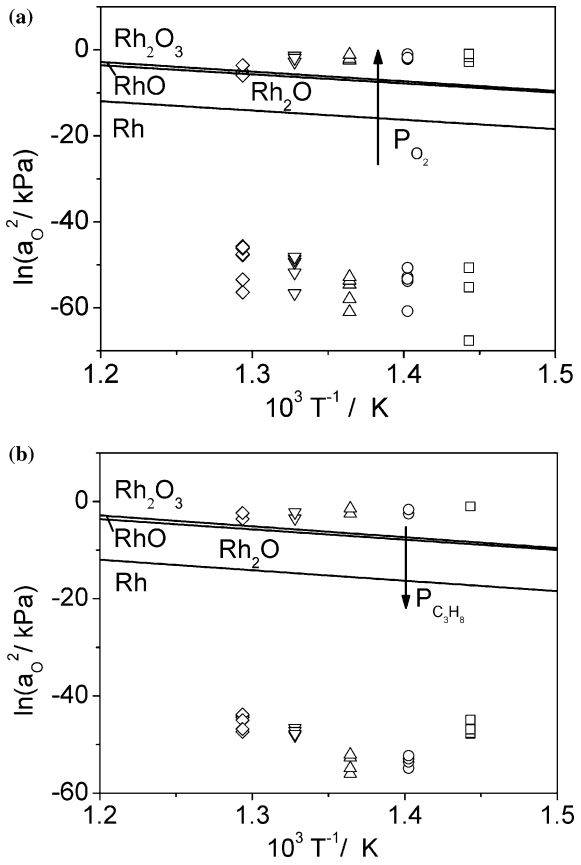

Fig. 8. Effect of temperature and gas phase composition on surface oxygen activity a_O and comparison with the oxygen activity values corresponding to the stability limits of bulk rhodium oxides [21]. (a) $P_{C_3H_8} = 2$ kPa (b) $P_{O_2} = 0.5$ kPa; Key for T: (□) 420 °C, (○) 440 °C, (△) 460 °C, (▽) 480 °C, (◇) 500 °C (see text for discussion).

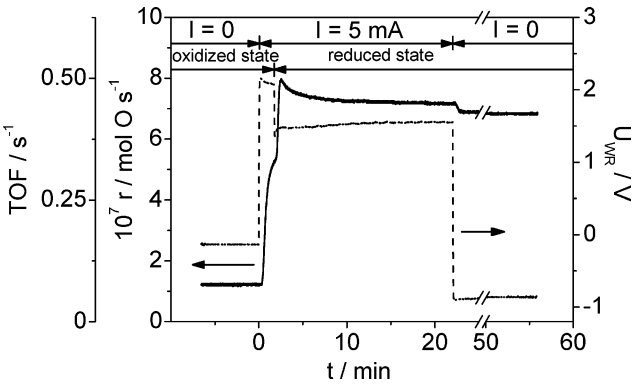

Fig. 9. Rate r, turnover frequency TOF and catalyst potential U_{WR} response to a step change in applied positive current. Catalyst Rh. $T = 500$ °C; Feed composition: $P_{O_2} = 1.8$ kPa, $P_{C_3H_8} = 2$ kPa; Flow rate: 83 cm^3 (STP) min^{-1} (see text for discussion).

$P_{O_2,R} \approx 21$ kPa $= 0.21$ bar). At each temperature in Figure 8 it is clearly seen the abrupt transition from a reduced to an oxidized state by increasing the oxygen partial pressure (Figure 8a) or by decreasing the propane partial pressure (Figure 8b).

Figure 9 shows for catalyst Rh at 500 °C a galvanostatic transient, that is, the response of the catalyst potential U_{WR} and of rate r (expressed in mol O s^{-1}) and turnover frequency (TOF) of propane oxidation upon application of a constant positive current of 5 mA between the rhodium catalyst and the Pt counter electrode. Upon current application the catalytic rate, equal at open-circuit to $r_o = 1.2\times10^{-7}$ mol O s^{-1}, starts increasing gradually but after a few minutes an abrupt increase in the rate is observed. Then the rate, after passing through a shallow maximum, stabilizes gradually to a steady-state value equal to 7.17×10^{-7} mol O s^{-1} which is six times higher than the open-circuit rate (rate enhancement ratio $\rho = r/r_o = 6$). The corresponding faradaic efficiency Λ value at steady-state is equal to 23. The aforementioned abrupt increase in the catalytic rate is accompanied by an abrupt decrease in catalyst potential by approximately 700 mV, which then gradually stabilizes to a value equal to 1.55 V. These abrupt changes in catalytic rate and catalyst potential indicate change in the oxidative state of the catalyst in agreement with former studies of oxidation reactions on Rh catalyst films [21, 24, 28] where it has been observed that application of currents or potentials can affect significantly the stability limit of the surface rhodium oxide. The catalyst surface changes from an oxidized to a reduced state upon application of positive current due to the fact that the induced increase in catalyst work function [2, 4, 5] results in weakening in the chemisorptive bond strength of electron acceptor adsorbates [4, 5, 19], such as dissociatively chemisorbed oxygen [5, 29], thus destabilizing surface rhodium oxide.

After current interruption the catalytic rate relaxes to a value $r' = 6.85\times10^{-7}$ mol O s^{-1}, which is approximately 5.7 times higher than the initial open-circuit rate while the potential relaxes to a value equal to −855 mV, which is lower than its initial open-circuit value ($U_{WR,o} = -135$ mV) by 720 mV. This shows that the catalyst remains in the reduced state after current interruption and a "permanent NEMCA behavior" [5, 30] is observed corresponding to a "permanent" rate enhancement ratio [30] $\gamma = r'/r_o \approx 5.7$. Oxidation of the catalyst under flow of 21% O_2 in He mixture for 1 h and subsequent feed of the reaction mixture resulted in attainment of practically the initial open-circuit rate and potential values.

Figure 10 shows the dependence of the rate r and turnover frequency (TOF) of propane oxidation on oxygen partial pressure P_{O_2}, at constant $P_{C_3H_8} = 2.2$ kPa and $T = 500$ °C, under open-circuit conditions and when the catalyst potential is maintained at 0.5 or 2 V (application of positive overpotentials). As shown in the figure, the kinetic effect of oxygen remains qualitatively the same under closed-circuit (EP) conditions, that is, the reaction mechanism does not change under conditions of EP. The value of the critical oxygen pressure $P^*_{O_2}$ beyond which the catalyst surface is oxidized increases with increasing catalyst potential. Similar to the case of ethylene oxidation on Rh/YSZ [21], this behavior can be explained by the induced, via application of positive overpotential, decrease in the

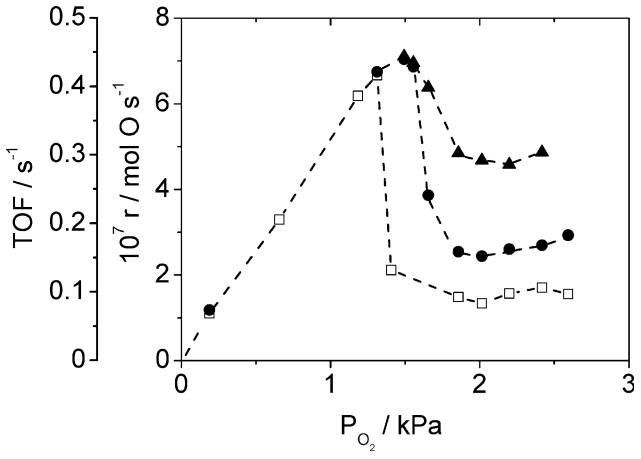

Fig. 10. Effect of P_{O_2} and imposed catalyst potential on the rate of propane oxidation (expressed in mol O s^{-1}) and turnover frequency (TOF). Catalyst Rh. $T = 500$ °C; $P_{C_3H_8} = 2.2$ kPa; Flow rate: 80–95 cm^3 (STP) min^{-1}; (□) open-circuit conditions, (●) $U_{WR} = 0.5$ V, (▲) $U_{WR} = 2$ V.

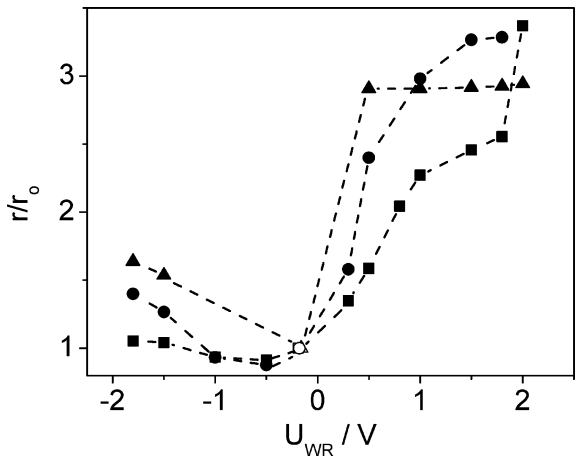

Fig. 11. Steady-state effect of applied catalyst potential on the catalytic rate enhancement ratio $\rho = r/r_o$ at different temperatures. Open symbols correspond to open-circuit conditions. Catalyst Rh; $P_{O_2} = 1.56$ kPa, $P_{C_3H_8} = 2.2$ kPa; Flow rate: 80–95 cm^3 (STP) min^{-1}; Key for T: (■) 460 °C ($r_o = 2.03\times10^{-7}$ mol O s^{-1}, $U_{WR,o} = -190$ mV), (●) 480 °C ($r_o = 2.27\times10^{-7}$ mol O s^{-1}, $U_{WR,o} = -178$ mV), (▲) 500 °C ($r_o = 2.36\times10^{-7}$ mol O s^{-1}, $U_{WR,o} = -161$mV).

chemisorptive bond strength of oxygen [4, 5, 21]. This weakening of the rhodium–oxygen bond and the also induced via application of positive overpotential increase in the chemisorptive bond strength of propane [5], which is an electron acceptor adsorbate [31], can explain the observed in Figure 10 increase in catalytic rate with increasing catalyst potential at constant P_{O_2} and $P_{C_3H_8}$.

Figure 11 shows for catalyst film Rh and for $P_{O_2}/P_{C_3H_8} \approx 0.7$ the steady-state effect of applied potential U_{WR} on the catalytic rate enhancement ratio $\rho = r/r_o$ in the temperature range 460–500 °C. Similar to the case of Pt/YSZ, the dependence of catalytic rate on applied potential exhibits an "inverted volcano type" behavior. The rate minimum in this case appears to be shifted to potentials more negative than the open-circuit potential, however the corresponding rate decrease was minimal and did not exceed 13%. Compared to the Pt/YSZ system (Figure 4), the observed rate enhancement is not that significant as the highest rate enhancement ratio $\rho = r/r_o$ did not exceed 3.4 for positive overpotentials and 1.7 for negative overpotentials. The maximum propane conversion observed here under potential application was 5.1% (at 480 °C) at a flow rate equal to 87 cm^3 (STP) min^{-1}.

Figure 12 shows for catalyst film Rh and for the conditions of Figure 11 the steady-state effect of applied current I or, equivalently, of corresponding rate $I/2F$ of O^{2-} transfer through the solid electrolyte on the observed change in the catalytic rate Δr of propane oxidation (expressed as O consumption, in mol O s^{-1}). The electrochemically induced rate changes are non-faradaic with corresponding values of faradaic efficiency Λ between −25 and 830. The highest value of Λ ($\Lambda = 830$) was measured at 460 °C for application of +300 mV corresponding to a current of 16.5 μA.

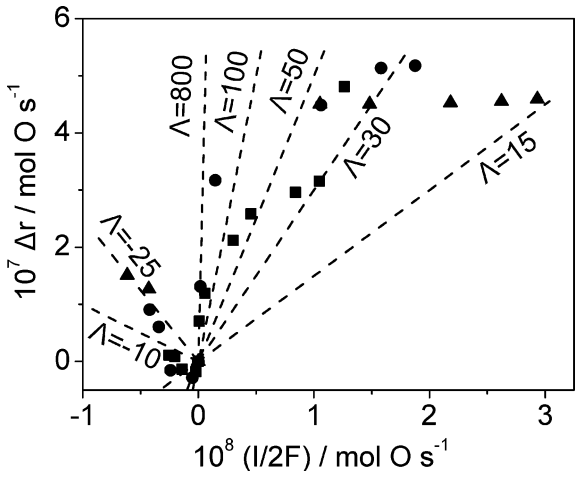

Fig. 12. Steady-state effect of applied current I on the induced change in the rate of propane oxidation Δr (expressed in mol O s^{-1}). Dashed lines are constant Faradaic efficiency Λ lines. Catalyst Rh. Conditions as in Figure 11.

4. Discussion

The observed EP behavior for both the Pt and Rh catalysts can be explained in the frame of the general principles concerning the origin of the EP effect [4, 5], in view of the mechanism of the reaction and the relative strength of the chemisorptive bonds of the adsorbed reactants. Propane and oxygen adsorb competitively on the metal catalyst surface [9, 13, 18] and as a result a Langmuir–Hinshelwood type kinetic behavior is observed [18]. Oxygen is more strongly adsorbed on Pt surfaces compared to propane [9, 18, 32, 33] and the same is expected for Rh surfaces as in general oxygen is

more strongly adsorbed on metal surfaces compared to alkanes [33]. This difference in chemisorptive bond strength, in view of the Langmuir–Hinshelwood mechanism, explains why always positive reaction orders with respect to propane have been reported [8, 9, 13, 34] while zero or negative reaction orders have been typically reported with respect to oxygen [8, 9, 13, 34]. The reaction orders have been found to depend not only on gas phase composition and temperature but also on the support [13, 34] and the metal catalyst oxidative state [13], mainly referring to supported platinum catalysts. Large differences also in the turnover frequencies (TOF) have been reported for platinum catalysts supported on different supports in the presence or absence of additives [6, 11, 14, 34].

The EP experiments presented in this study were carried out at relatively high temperatures ($T > 420$ °C) and at $P_{O_2}/P_{C_3H_8}$ ratios below the stoichiometric ratio. As a result the coverages of the reactants can be assumed to be relatively low, with the propane coverage being much lower than the oxygen coverage. Thus either positive or negative overpotential application is expected to enhance the rate [5, 22] as it will result in strengthening of the chemisorptive bond strength of either propane (electron donor [31]) or oxygen (electron acceptor [5, 29]), respectively, and in increase of the corresponding coverage. As oxygen is more strongly adsorbed on the catalyst surface compared to propane, weakening of its chemisorptive bond upon application of positive overpotentials is in general expected to have the most significant impact on the rate (Figures 4a and 11). The presence of propane has no significant effect on the chemisorptive bond strength of the electrochemically pumped ionic promoting oxygen species [32] which are responsible for the catalyst work function change [2, 4, 5] and the alteration of the strength of the chemisoptive bond of the normally chemisorbed reactive oxygen [5, 19, 23]. The difference in the relative strength of the chemisorptive bonds of the adsorbed reactants on Pt and Rh can also explain the lower rate enhancement ratios observed in the case of Rh. It is well established that oxygen is strongly bonded onto the Rh surface forming stable metal oxide layers [24, 35–37], the presence of which results in decrease of the catalytic activity, e.g. for hydrocarbon oxidation [21, 24]. Surface PtO_2 can also be formed by interaction of oxygen with platinum surfaces [4, 5, 38] however it is less stable compared to surface rhodium oxides and more easily decomposed [27]. Due to the stronger bonding of oxygen on the rhodium surface the relative effect of altering catalyst potential and work function on the strength of the metal–oxygen bond is expected to be not so pronounced as in the case of Pt, which can explain why the observed EP effect is less pronounced in the case of Rh.

The oxidative state of the catalyst and its dependence on reaction conditions and applied catalyst potential is also an important parameter in explaining similarities and differences in the observed EP behavior between Pt and Rh and under different $P_{O_2}/P_{C_3H_8}$ ratios. The large difference in the open-circuit potential of the Pt catalyst films under the conditions of Figures 3a and 4a on one side ($U_{WR,o}$ from −371 to −448 mV) and Figures 3b and 4b on the other side ($U_{WR,o}$ from 5 to 90 mV) reflects a difference in the oxidative state of the catalyst. The catalyst surface (catalyst Pt2) is oxidized in the latter case, as can be deduced by comparing the oxygen activity values corresponding to the stability limit of PtO_2 [27] with the ones corresponding to $U_{WR,o}$ (Figures 3b and 4b) and calculated from Equation (2). The fact that the platinum surface is oxidized under these conditions (Figures 3b and 4b) is corroborated by the low values of the open-circuit catalytic rate, in view of the fact that oxidation of the platinum surface results in decrease of the catalytic activity for propane combustion [11, 39]. Oxidized state of the platinum catalyst surface has also been reported in the case of propane oxidation on Pt/YSZ between 250 and 450 °C under oxygen-rich or stoichiometric conditions [32]. The quite pronounced, in terms of rate enhancement ratios, electrochemical promotion observed with platinum catalyst film Pt2 under the conditions of Figures 3b and 4b ($P_{O_2}/P_{C_3H_8} \approx 3.1$ to 3.4, $T = 480$–520 °C) and the similar rate enhancement ratios observed in this case for positive and negative overpotential application can be attributed to a large extent to decomposition of the surface platinum oxide, in view of the fact that metallic platinum shows higher activity for propane combustion [11, 39]. This explanation is in agreement with the observed increase, under oxidizing conditions, in the catalytic activity for propane combustion of supported platinum catalysts via addition of electronegative additives [14], which has been attributed to the increase in the oxidation-resistance of the platinum catalyst. The decomposition of the surface platinum oxide under positive overpotential application can be explained by the induced increase in catalyst work function [2, 4, 5] and the concomitant weakening in the chemisorptive bond strength of oxygen [4, 5, 19, 23] and decrease in the stability of surface platinum oxide against reduction. The appearance of maximum in the rate transient depicted in Figure 3b can be attributed to oxygen resulting from the decomposition of surface platinum oxide following positive current application. The decomposition of the surface platinum oxide under negative overpotential application can be simply explained by electrochemical reduction of surface platinum oxide:

$$Pt^{4+} + 4e^- \rightarrow Pt^0 \qquad (3)$$

Electrochemical reduction of the surface oxide has been used to explain the activation via application of negative currents of rhodium catalyst films interfaced to TiO_2/YSZ with respect to the partial oxidation of methane to syngas [28].

In the case of rhodium catalyst the observed EP behavior can also be attributed to a large extent to

changes in the oxidative state of the catalyst, i.e. to the effect of catalyst potential on the stability limit of surface rhodium oxides. In both the transient (Figure 9) and steady-state (Figure 11) EP experiments presented here the rhodium catalyst under open-circuit conditions was oxidized but close to the limit of surface reduction (Figures 6 and 10). Under positive current application the catalyst becomes reduced and thus more active due to the weakening of the rhodium–oxygen bonding strength as a result of the electrochemically induced oxygen ion backspillover onto the catalyst surface and the concomitant increase in surface work function [5, 21, 24]. This is corroborated by the fact that the maximum rate enhancement ratio shown in Figure 11 for positive overpotential application at 500 °C, equal to 2.95, is very close to the ratio 3.2 of the open-circuit rates corresponding to the oxidized and the reduced states of the catalyst at the same temperature (Figure 10). This effect of oxygen ion backspillover on the stability of surface rhodium oxide can also partly explain the higher rate enhancement ratios observed in the case of rhodium catalyst upon positive overpotential application, in addition to the difference in the binding strengths of oxygen and propane, assuming that in the case of rhodium catalyst the electrochemical reduction of surface rhodium oxides (which are more stable than surface platinum oxide [27]) via negative overpotential application is less effective compared to the decomposition of surface rhodium oxides induced by the presence of the backspillover oxygen ionic species.

Besides changes in the coverage of the chemisorbed reactants, changes in the binding strength of the chemisorbed reactive species as a result of changes in catalyst potential is also expected in general to affect both the apparent activation energy of the catalytic reaction, if the rate determining step (rds) involves cleavage of chemisorptive bonds, and the apparent pre-exponential factor, which depends on the mobility and relative amounts of chemisorbed reactants [4, 5, 19, 21]. The rate determining step (rds) in propane combustion mechanism over metal catalysts is considered to be the dissociative chemisorption of propane accompanied by C–H bond cleavage [7–9, 34, 40], as expected by the low sticking probability of alkanes on metals [8]. This is reflected on the first order kinetics in propane reported in literature [8, 9, 13, 34]. The strengthening of the propane-metal bond due to application of positive overpotentials and concomitant transfer on the gas exposed catalyst surface of promoting ionic oxygen species from the solid electrolyte is expected to result in easier activation of the C–H bond in the rds and thus affect the activation energy of the reaction, which can also partly explain the observed more pronounced rate increase for application of positive currents (Figures 4a and 11). The interaction of the ionic backspillover oxygen with adsorbed propane may also facilitate the initial C–H bond activation in a manner similar to the one proposed by Burch et al. [9] in order to interpret the promotion of propane oxidation by SO_2 over supported Pt catalysts.

Concerning the case of Pt catalyst, the present results, although they show an ''inverted volcano type'' dependence of catalytic rate on catalyst potential, do not contradict the results of Vernoux et al. [18] who reported electrophobic NEMCA behavior for the same reaction, that is, increase in the rate of propane oxidation upon positive overpotential application and decrease upon negative overpotential application. In this case the experiments were carried out at not only at a lower temperature ($T = 344$–365 °C) but also at a much lower propane partial pressure ($P_{C_3H_8} = 0.2$ kPa) and a higher $P_{O_2}/P_{C_3H_8}$ ratio (5–12.5), that is, under conditions where the catalyst surface is mainly covered by oxygen, the electron acceptor reactant, and thus electrophobic behavior is expected according to the rules of promotion that were recently derived by Vayenas and coworkers [5, 22, 23] for predicting the promotion and EP behavior. Such changes from ''inverted volcano'' to electrophobic EP behavior have been experimentally observed [41] but also theoretically modeled and predicted [23].

5. Conclusions

The present study shows that EP can dramatically affect the complete oxidation of propane on Pt or Rh films interfaced to YSZ. In the temperature range 420–520 °C and for sub-stoichiometric $P_{O_2}/P_{C_3H_8}$ ratios the rate of propane combustion is enhanced upon application of either positive or negative overpotential or current (''inverted volcano'' behavior), by up to 1350 times in the case of Pt and by up to a factor of 6 in the case of Rh. The observed rate changes are strongly non-faradaic exceeding the corresponding electrocatalytic rate by up to 2330 times in the case of Pt and by up to 830 times in the case of Rh. The promotional behavior can be explained taking into account the mechanism of the reaction and the effect of catalyst potential on the binding strength of chemisorbed reactants and on the oxidative state of the catalyst surface.

Acknowledgments

The authors thank the European Social Fund (ESF), Operational Program for Educational and Vocational Training II (EPEAEK II) and particularly the Program IRAKLEITOS, for financially supporting this work. They also thank Dr V. Drakopoulos, Institute of Chemical Engineering and High Temperature Chemical Processes (ICE-HT/FORTH) for the scanning electron microscopy (SEM) characterization of the catalyst-electrodes.

References

1. J. Pritchard, *Nature* **343** (1990) 592.
2. C.G. Vayenas, S. Bebelis and S. Ladas, *Nature* **343** (1990) 625.
3. C.G. Vayenas, S.I. Bebelis and S. Neophytides, *J. Phys. Chem.* **92** (1988) 5083.
4. C.G. Vayenas, M.M. Jaksic, S. Bebelis and S.G. Neophytides *in* J.O'M. Bockris, B.E. Conway and E. White (Eds), Modern Aspects of Electrochemistry 29, (Plenum, New York, 1996), pp. 57–202.
5. C.G. Vayenas, S. Bebelis, C. Pliangos, S. Brosda and D. Tsiplakides, *Electrochemical Activation of Catalysis* (Kluwer Academic Publishers/Plenum Press, New York, 2001).
6. C.P. Hubbard, K. Otto, H.S. Gandhi and K.Y.S. Ng, *J. Catal.* **139** (1993) 268.
7. A. Hinz, M. Skoglundh, E. Fridell and A. Andersson, *J. Catal.* **201** (2001) 247.
8. M. Aryafar and F. Zaera, *Catal. Lett.* **48** (1997) 173.
9. R. Burch, E. Halpin, M. Hayes, K. Ruth and J.A. Sullivan, *Appl. Catal. B* **19** (1998) 199.
10. K. Wilson, C. Hardacre and R.M. Lambert, *J. Phys. Chem.* **99** (1995) 13755.
11. Y. Yazawa, N. Takagi, H. Yoshida, S. Komai, A. Satsuma, T. Tanaka, S. Yoshida and T. Hattori, *Appl. Catal. A* **233** (2002) 103.
12. Y. Yazawa, H. Yoshida and T. Hattori, *Appl. Catal. A* **237** (2002) 139.
13. Y. Yazawa, N. Kagi, S. Komai, A. Satsuma, Y. Murakami and T. Hattori, *Catal. Lett.* **72** (2001) 157.
14. Y. Yazawa, H. Yoshida, S. Komai and T. Hattori, *Appl. Catal. A* **233** (2002) 113.
15. P. Tsiakaras and C.G. Vayenas, *J. Catal.* **140** (1993) 53.
16. A.D. Frantzis, S. Bebelis and C.G. Vayenas, *Solid State Ionics* **136–137** (2000) 863.
17. A. Kaloyannis and C.G. Vayenas, *J. Catal.* **171** (1997) 148.
18. P. Vernoux, F. Gaillard, L. Bultel, E. Siebert and M. Primet, *J. Catal.* **208** (2002) 412.
19. S. Bebelis and C.G. Vayenas, *J. Catal.* **118** (1989) 125.
20. I.V. Yentekakis and S. Bebelis, *J. Catal.* **137** (1992) 278.
21. C. Pliangos, I.V. Yentekakis, X.E. Verykios and C.G. Vayenas, *J. Catal.* **154** (1995) 124.
22. C.G. Vayenas, S. Brosda and C. Pliangos, *J. Catal.* **203** (2001) 329.
23. S. Brosda and C.G. Vayenas, *J. Catal.* **208** (2002) 38.
24. G. Fóti, I. Bolzonella, D. Bachelin and Ch. Comninellis, *J. Appl. Electrochem.* **34** (2004) 9.
25. L. Riekert, *Ber. Bunsenges. Phys. Chem.* **85** (1981) 297.
26. R. Wüthrich, E.A. Baranova, H. Bleuler and Ch. Comninellis, *Elec. Commun.* **6** (2004) 1199.
27. M. Peuckert, *J. Phys. Chem.* **89** (1985) 2481.
28. E.A. Baranova, G. Fóti and Ch. Comninellis, *Elec. Commun.* **6** (2004) 389.
29. M.P. Kiskinova *in* B. Delmon and J.T. Yates (Eds), Studies in Surface Science and Catalysis 70, (Elsevier B.V., Amsterdam, 1992).
30. J. Nicole, D. Tsiplakides, S. Wodiunig and Ch. Comninellis, *J. Electrochem. Soc.* **144** (1997) L312.
31. Z. Hlavathy and P. Tétényi, *Surf. Sci.* **410** (1998) 39.
32. L. Bultel, C. Roux, E. Siebert, P. Vernoux and F. Gaillard, *Solid State Ionics* **166** (2004) 183.
33. R. Burch, D.J. Crittle and M.J. Hayes, *Catal. Today* **47** (1999) 229.
34. T.F. Garetto, E. Rincón and C.R. Apesteguía, *Appl. Catal. B* **48** (2004) 167.
35. G.L. Kellog, *Surf. Sci.* **171** (1986) 359.
36. S.H. Oh and J.E. Carpenter, *J. Catal.* **80** (1983) 472.
37. A.D. Logan, A.K. Datye and J.E. Houston, *Surf. Sci.* **245** (1991) 280.
38. M. Peuckert and H.P. Bonzel, *Surf. Sci.* **145** (1984) 239.
39. H. Yoshida, Y. Yazawa and T. Hattori, *Catal. Today* **87** (2003) 19.
40. R. Burch and T.C. Watling, *J. Catal.* **169** (1997) 45.
41. C. Pliangos, I.V. Yentekakis, S. Ladas and C.G. Vayenas, *J. Catal.* **159** (1996) 189.